# Theoretical study for water structure at highly ordered surface: Effect of surface structure

Ryo Akiyama and Fumio Hirata

Citation: The Journal of Chemical Physics **108**, 4904 (1998); doi: 10.1063/1.475899
View online: http://dx.doi.org/10.1063/1.475899
View Table of Contents: http://scitation.aip.org/content/aip/journal/jcp/108/12?ver=pdfcov
Published by the AIP Publishing

# Theoretical study for water structure at highly ordered surface: Effect of surface structure

Ryo Akiyama and Fumio Hirata
*Institute for Molecular Science, Myodaiji, Okazaki 444, Japan*

(Received 22 August 1997; accepted 19 December 1997)

The structure of water at an ordered solid surface is investigated by the reference interaction site method (RISM). A RISM equation devised especially for a solute–solvent system in which the solute is a two-dimensional periodic array is employed to formulate the electrode–solution interface. Calculations are carried out for two types of surfaces: flatlike and Au(111)-like structures. The orientation of water molecules at the Au(111)-like surface with various surface charge densities, which are deduced from the correlation functions, is in good agreement with the results of surface-enhanced infrared absorption spectroscopy. On the other hand, the model of the flatlike surface does not give a consistent picture with the experiments. The difference is significant when the walls are negatively charged. In the case of a negatively charged wall, the Au(111)-like model gives about 108° for the angle between the surface normal vector and the two O–H vectors of the water molecules in the first layer, whereas the angles are about 72° and 180° for the flatlike surface. The results demonstrate that the solid surface structure is very important in discussing the structure and orientation of water molecules at the interface. © *1998 American Institute of Physics*. [S0021-9606(98)51612-1]

## I. INTRODUCTION

Due to recent progress in experimental techniques in *in situ* measurements, electrochemistry seems to be making a new epoch in understanding the chemical processes at electrode–solution interfaces. The new technology includes the scanning tunneling microscope (STM) extended to the solution phase[1–10] and surface enhanced infrared absorption spectroscopy.[11–17] These methods are revealing the structure of the electrode surface as well as configurations of adsorbed species in atomic detail.[1–17] The information at atomic level has been combined with the traditional techniques in electrochemistry such as the cyclic voltammogram to provide a more complete picture of electrode–solution interfaces. Obviously, the traditional descriptions using electric double layer models, which are based on continuum models of the solvent, misfit the level of detail attained by recent experimental techniques.[18–21]

Theoretical understanding of the interface has also made great progress in the last two decades,[21–37] especially in terms of solvent configuration near electrode surfaces.[25–37] The progress has been mainly driven by two theoretical methods in the statistical mechanics of liquids: the molecular simulation and the integral equation methods. The two methods have reached consistent molecular pictures regarding reorganization of the water structure in the vicinity of the flat electrode surface.[30,35–37] The latest topics in those approaches concern the electronic structure of electrode. The method features a self-consistent treatment of the liquid state and the electronic structure of the metal surface.[32–34] The significance of such treatments will become more and more clear as the methods are extended to include chemical reactions at the interface, which are a primary motivation for electrochemistry.

Although the integral equation methods have great advantage in the overall description of the electrode–solution interface both at phenomenological and molecular levels, the models which have been employed for the metal surface seem oversimplified considering the resolution attained by the latest developments in experimental techniques stated above. The large sphere models which have been employed by Patey's group and others for representing the flat electrode surface, fit quite well in the theoretical framework of the RHNC equations.[38,39] However, the models have obvious difficulty in being extended to a structured surface. The treatment by Blum and co-workers, which uses a sticky-site description for the metal surface,[21–24] is succesfull in explaining the adsorption of ions at an ordered metal surface, but it has its own disadvantage of oversimplifying the solvent as a dielectric continuum. Here, we propose a new approach for the electrode–solution interface based on the reference interaction site method (RISM) of liquids,[40–42] which can handle both the structured metal surface and water in atomic level.

The RISM equation is succesfull in describing a large variety of chemical processes in solution in atomic detail.[40–49] An application of the theory to the electrode–solution interface, however, is not so straightforward due to the large number of atomic sites which represent a metal surface.[46,47] Namely, we have to solve as many as $n \times m$ coupled integral equations, where $n$ and $m$ are the number of atomic sites in the metal surface and that of a solvent molecule, respectively. Fortunately, when the configuration of atoms in the metal surface has some periodicity, the number of equations can be drastically reduced as has been done for periodic polymers in solution.[46–49] In the present study, we employ the idea to facilitate an atomic description of electrode–solution interfaces.

 

## II. THEORY

In this article, we treat the system of an ordered surface in liquid water. We regard the surface which is a two-dimensional array as a single solute molecule at infinite dilution in a solvent. This solute–solvent system is treated by the RISM equation and a HNC-type closure relation.

The RISM equation[40–42] is written in the most general form as

$$\boldsymbol{\rho}\mathbf{h}\boldsymbol{\rho}=\boldsymbol{\omega}*\mathbf{c}*\boldsymbol{\omega}+\boldsymbol{\omega}*\mathbf{c}*\boldsymbol{\rho}\mathbf{h}\boldsymbol{\rho}, \tag{1}$$

where $\mathbf{h}$ is the matrix of site–site intermolecular pair correlation functions, $\mathbf{c}$ is the matrix of direct correlation functions. ''*'' denotes a matrix convolution product. The $\omega$ is an intramolecular correlation matrix defined as

$$\omega_{\alpha_M\gamma_{M'}}(|\mathbf{r}-\mathbf{r}'|)=\rho_M\delta_{MM'}[\delta_{\alpha_M\gamma_{M'}}\delta(\mathbf{r}-\mathbf{r}') +(1-\delta_{\alpha_M\gamma_{M'}})s_{\alpha_M\gamma_{M'}}(|\mathbf{r}-\mathbf{r}'|)], \tag{2}$$

where $s$ is the intramolecular distribution function between site $\alpha$ and site $\gamma$, which is a Dirac delta function for a rigid bond as

$$s_{\alpha_M\gamma_{M'}}(|\mathbf{r}-\mathbf{r}'|)=(1/4\pi L^2_{\alpha_M\gamma_{M'}})\,\delta(|\mathbf{r}-\mathbf{r}'|-L_{\alpha_M\gamma_{M'}}). \tag{3}$$

$L_{\alpha_M\gamma_M}$ is the distance between sites $\alpha_M$ and $\gamma_M$. $M$ (or $M'$) means molecular species and $\delta_{MM'}$, etc., is a Kronecker delta. $\rho$ is a diagonal matrix composed of the densities of the constituent species,

$$\rho_{\alpha_M\gamma_{M'}}=\delta_{\alpha_M\gamma_{M'}}\rho_M, \tag{4}$$

where $\rho_M$ is the number density of molecular species $M$.

For applying the theory to the electrode–solution interface, we regard the electrode as a solute molecule in solution at infinite dilution. Through a limiting process of vanishing solute density, Eq. (1) can be rearranged in terms of solvent–solvent and solute–solvent equations as,

$$\mathbf{h^{vv}}=\mathbf{w^v}*\mathbf{c^{vv}}*\mathbf{w^v}+\mathbf{w^v}*\mathbf{c^{vv}}*\boldsymbol{\rho}\mathbf{h^{vv}}, \tag{5}$$

$$\mathbf{h^{uv}}=\mathbf{w^u}*\mathbf{c^{uv}}*\mathbf{w^v}+\mathbf{w^u}*\mathbf{c^{uv}}*\boldsymbol{\rho}\mathbf{h^{vv}}, \tag{6}$$

where superscripts $u$ and $v$ mean solute (electrode) and solvent, respectively.[42] The matrix $\mathbf{w}$ is defined with solvent density $\rho$ by

$$\boldsymbol{\omega}=\boldsymbol{\rho}\mathbf{w}. \tag{7}$$

As can be easily seen from Eq. (6), the straightforward application of the theory to the electrode–solution interface is difficult since the number of coupled equations to be solved amounts to $n\times m$ with $n$ being infinitely large, where $n$ and $m$ are the number of atomic sites in the electrode and a solvent molecule. However, in such a case where atoms in the solute are arranged in a periodic array, the number of equations can be reduced drastically as has been done in the case of a periodic polymer.[46,47] Indeed, atoms in the electrode surface can be regarded as being in a periodic array, which fits nicely to the theory. In order to take advantage of the periodicity of the electrode surface, we rewrite Eq. (6) as,

$$h^{uv}_{\alpha_i\beta_M}(|\mathbf{r}-\mathbf{r}'|)=\sum_{\zeta_{M'}}\sum_j\sum_\gamma\int\int d\mathbf{r}_1d\mathbf{r}_2w^u_{\alpha_i\gamma_j}(|\mathbf{r}-\mathbf{r}_1|) \times c^{uv}_{\gamma_j\zeta_{M'}}(|\mathbf{r}_1-\mathbf{r}_2|)[w^v_{\zeta_{M'}\beta_M}(|\mathbf{r}_2-\mathbf{r}'|) +\rho h^{vv}_{\zeta_{M'}\beta_M}(|\mathbf{r}_2-\mathbf{r}'|)], \tag{8}$$

where $\alpha$, $\beta$, $\gamma$, $\zeta$ are the atomic sites in the electrode and a solvent molecule. The subscripts $i$ and $j$ represent periodic units in the surface, namely, $\alpha_i$ is the $\alpha$th site in the $i$th unit. $\mathbf{w^u}$ is also rewritten in terms of the periodic units,

$$w^u_{\alpha_i\gamma_j}(|\mathbf{r}-\mathbf{r}'|)=\delta_{\alpha_i\gamma_j}\delta(\mathbf{r}-\mathbf{r}')+(1-\delta_{\alpha_i\gamma_j}) \times(1/4\pi L^2_{\alpha_i\gamma_j})\,\delta(|\mathbf{r}-\mathbf{r}'|-L_{\alpha_i\gamma_j}). \tag{9}$$

Since the surface sites have periodicity, $\mathbf{h^{uv}}$ and $\mathbf{c^{uv}}$ should be identical for each of the units if the electrode extends infinitely in the two dimensions, namely,

$$c^{uv}_{\gamma_j\zeta_{M'}}(|\mathbf{r}-\mathbf{r}'|)=c^{uv}_{\gamma\zeta_{M'}}(|\mathbf{r}-\mathbf{r}'|)(j=0,1,2,3,...). \tag{10}$$

By carrying out the summation on $j$, Eq. (8) gives

$$h^{uv}_{\alpha_i\beta_M}(|\mathbf{r}-\mathbf{r}'|)=\sum_{\zeta_{M'}}\sum_\gamma\int\int d\mathbf{r}_1d\mathbf{r}_2W^u_{\alpha_i\gamma}(|\mathbf{r}-\mathbf{r}_1|) \times c^{uv}_{\gamma\zeta_{M'}}(|\mathbf{r}_1-\mathbf{r}_2|)[w^v_{\zeta_{M'}\beta_M}(|\mathbf{r}_2-\mathbf{r}'|) +\rho h^{vv}_{\zeta_{M'}\beta_M}(|\mathbf{r}_2-\mathbf{r}'|)], \tag{11}$$

where the intramolecular (surface) correlation function $W^u_{\alpha_i\gamma}$ is defined by

$$W^u_{\alpha_i\gamma}=\sum_j w^u_{\alpha_i\gamma_j}. \tag{12}$$

Since each periodic unit has identical structure, Eq. (11) consists of only $s\times m$ coupled equations, where $s$ is now the number of sites in a periodic unit. In actual implementation of the theory, the summation in Eq. (12) should be truncated at some distance between atomic sites. Although the approximation introduces some end effects, the error can be minimized by careful consideration of the correlation length. Equation (11) can be solved with a HNC-type closure relations using an iterative scheme.[47] The closure relation is written as

$$c^{uv}_{\gamma\zeta_{M'}}=\exp[-u_{\gamma\zeta_{M'}}/k_BT+h^{uv}_{\gamma\zeta_{M'}}-c^{uv}_{\gamma\zeta_{M'}}]-h^{uv}_{\gamma\zeta_{M'}} +c^{uv}_{\gamma\zeta_{M'}}-1, \tag{13}$$

where $u_{\gamma\zeta_{M'}}$ is the interaction between sites $\gamma$ and $\zeta_{M'}$.

## III. MODEL

The site–site interactions are represented by the (12-6-1) potential for both solvent–solvent and electrode–solvent atom pairs,

$$u_{\alpha\gamma}=4\epsilon_{\alpha\gamma}\left[\left(\frac{\sigma_{\alpha\gamma}}{r}\right)^{12}-\left(\frac{\sigma_{\alpha\gamma}}{r}\right)^{6}\right]+\frac{q_\alpha q_\gamma}{r}, \tag{14}$$

where $\sigma$ is the Lennard-Jones (L-J) diameter and $\epsilon$ is the value of energy minimum. The standard mixing rules

TABLE I. Geometrical and (1-6-12) potential parameters (Refs. 50, 51).

| Geometical parameters (X–X: First neighbor of surface atom) | | | |
|---|---|---|---|
| Bond | | length (Å) | |
| O–H(Water) | | 1.0 | |
| H–H(Water) | | 1.633 | |
| X–X(Type 1) | | 2.92 | |
| X–X(Type 2) | | 1.46 | |
| (1-6-12) potential parameters | | | |
| atom | $q$ | $\sigma$(Å) | $\epsilon$(erg.) |
| H(Water) | 0.41 | 1.0 | $3.79\times10^{-15}$ |
| O(Water) | $-0.82$ | 3.166 | $1.08\times10^{-14}$ |
| X(Surface atom) | - | 2.68 | $1.08\times10^{-16}$ |

$$\sigma_{\alpha\gamma}=(\sigma_\alpha+\sigma_\gamma)/2, \tag{15}$$

$$\epsilon_{\alpha\gamma}=\sqrt{\epsilon_\alpha\epsilon_\gamma} \tag{16}$$

are used, where $\alpha$ and $\gamma$ specify the sites, and $r$ is the separation between the two sites. The energy parameters as well as those defining the molecular and surface geometries are shown in Table I. We employ the SPC model[50] for a water molecule. The water model has three interaction sites. One of them has a charge of $-0.82$ in electronic units, which is the oxygen site with L-J radii of 1.583 Å. The others represent hydrogen sites which have charges of $+0.41$ and L-J radius of 0.5 Å. The distances of oxygen–hydrogen and hydrogen–hydrogen site pairs are 1.0 and 1.633 Å, respectively. Non-Coulombic interactions associated with hydrogen atoms are regarded as negligible. The L-J diameter $\sigma$ of a surface Au atom is taken from the literature.[51] The L-J $\epsilon$ of a surface atom is very small and the interaction has little attractive part (soft-core-like interaction).

The electrode surface is represented by a two-dimensional array consisting of 121 identical atoms ($m=121$). The array is shown in Fig. 1. Therefore, the summation $j$ of Eq. (12) is carried out from 0 to 120 and $s=1$ (see Sec. II). Two models for the surface structure are studied. One has a geometry similar to an Au(111) electrode (Type 1) and the other is flatlike (Type 2). The surface atoms form a hexagonal lattice characterized by lattice constants. The lattice constant of type 1 is 2.92 Å, which is nearly equal to that of Au(111). Type 2 has lattice constant 1.46 Å. Since the L-J diameter $\sigma$ of the surface atom is equal to 2.68 Å, Type 2 surface is virtually flat. The calculations are carried out for the cases of various surface charge densities. The charge density is defined by total charge of the surface atoms per surface area. The charge $q$ of an each surface atom in the Coulomb part of the interaction in Eq. (14) is shown in Table II. The temperature is 298 K for all the cases studied.

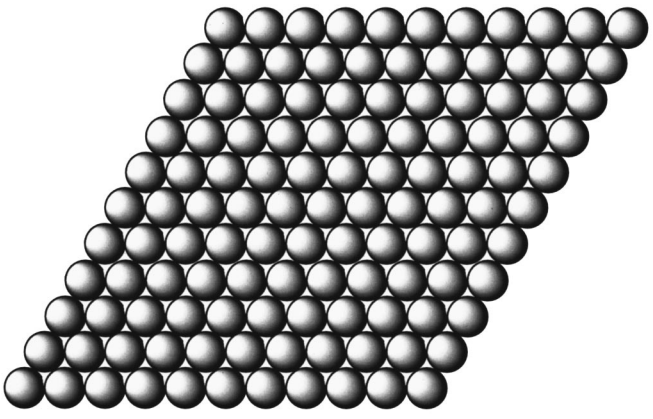

FIG. 1. Model of electrode surface.

TABLE II. Charge $q$ of each surface atom in the Coulomb part of (12-6-1) potential.

| Surface charge density ($C/m^2$) | $q$-Type 1 (electronic units) | $q$-Type 2 (electronic units) |
|---|---|---|
| 0.0 | 0.0 | 0.0 |
| $\pm0.1736$ | $\pm0.06612$ | $\pm0.01653$ |
| $\pm0.3472$ | $\pm0.1322$ | $\pm0.03306$ |
| $\pm0.5208$ | $\pm0.1983$ | $\pm0.04959$ |
| $\pm0.6944$ | $\pm0.2645$ | $\pm0.06612$ |
| $\pm0.8680$ | $\pm0.3306$ | $\pm0.08264$ |

As stated in the previous section, some caution should be made concerning the end effect of the correlation functions, which arises from the truncation of the intramolecular correlation matrix in Eq. (12). It was found that a model electrode with 11 atoms in an edge is sufficient to eliminate the end effect.

## IV. RESULT AND DISCUSSION

In this section, we show the surface atom(X)–solvent correlation function ($g(r)=h(r)+1$) and discuss the orientation of water molecules at the surface. Possible orientations of water molecules on the surface are illustrated in Fig. 2.

### A. Type 1 [Au(111)-like surface]

#### *1. Negatively charged surface*

We discuss the structure and orientation of water molecules at a negatively charged surface. Figure 3 shows the surface atom(X)–solvent correlation functions. In the case of surface charge density, $-0.868\ \mathrm{Cm}^{-2}$, the X–O correlation function [see Fig. 3(a)] has peaks around 2.5, 5.2, and 7.1 Å. Also, there is an appreciable shoulder around 4.2 Å. If oxygen atoms of water are placed on top of the surface atoms(X) [see Fig. 4(a)], it is predicted from simple consideration of geometry that the peaks should appear around 2.5, 3.8, 5.6, 6.4, and 8.1 Å (marked by white arrows). However, there are no peaks and no shoulders around 5.6, 6.4, and 8.1 Å. On the other hand, it is predicted that the peaks appear around 2.5, 3.8, 4.8, and 7.1 Å (marked by black arrows), when atoms in the Au(111)-like surface and water-oxygen atoms in the first layer form a closest packed structure. Namely, a water molecule sits on threefold hollow sites illustrated in Fig. 4(b). It seems that the shoulder around 4.2 Å at $q=-0.8680$ arises from the oxygen atoms which are expected to be at 3.8 Å and 4.8 Å if water molecules are sitting on the threefold hollow sites. Other positions are in good agreement with the peak positions of the correlation function. Therefore, it is reason-

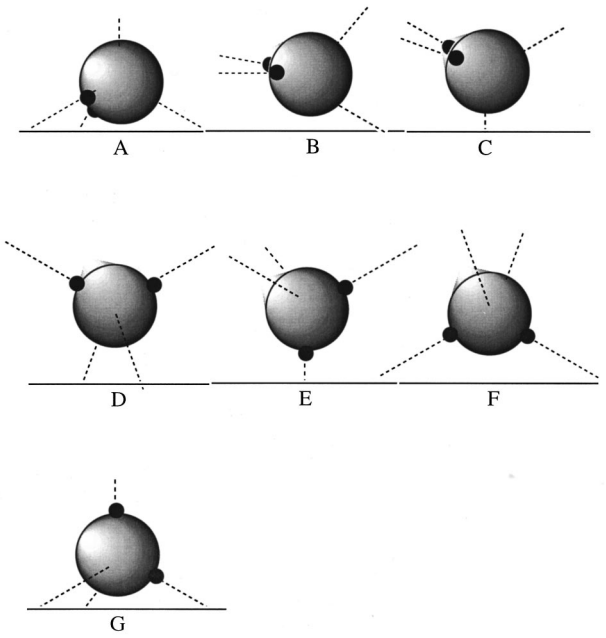


FIG. 2. Possible orientations of water molecule at the surface (solid lines). The large shaded and small black spheres represent oxygen and hydrogen atoms, respectively.

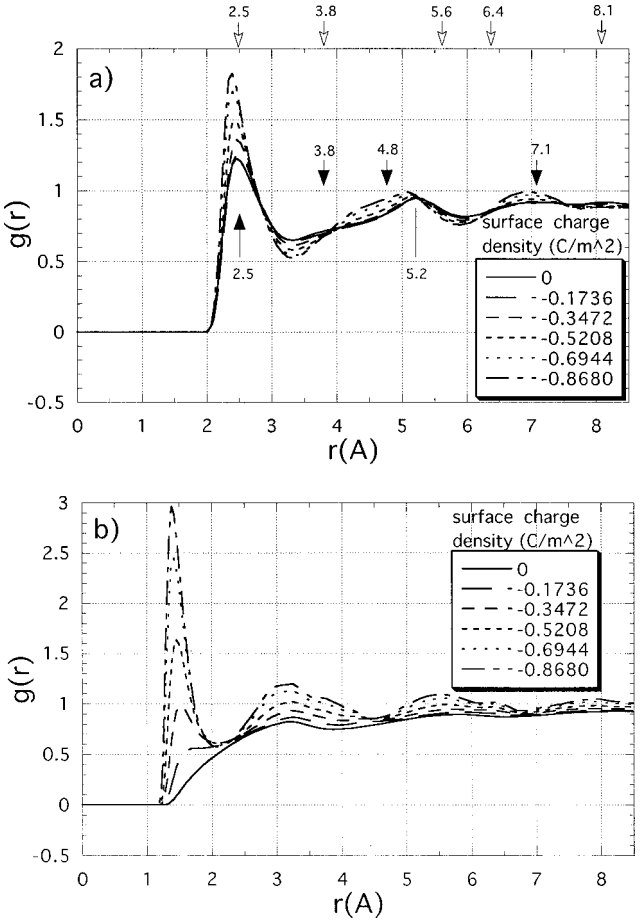


FIG. 3. The correlation functions between a surface atom (X) and water molecules at neutral and negatively charged Au(111) like surface (Type 1). (a) Surface atom (X)–oxygen correlation functions. If oxygen atoms of water molecules are placed on top of the surface atoms (X), it is predicted that the peaks appear around 2.5, 3.8, 5.6, 6.4 and 8.1 Å (marked by white arrows). On the other hand, it is predicted that the peaks appear around 2.5, 3.8, 4.8 and 7.1 Å (marked by black arrows), when the atoms in Au(111)-like surface and the water-oxygen atoms in the first layer form the closest packed structure. The peak of X–O correlation function around 5.2 Å can be assigned to water molecules in the second layer. (b) The first peak in the X–H correlation function is located at shorter distance than in the X–O correlation function. The difference of the peak positions is about 1 Å.

able to assign the latter structure, in which each water molecule of the first layer is located on threefold hollow sites, to the correlation functions.

The first peak in the X–H correlation function is located at a shorter distance than in the X–O function (see Fig. 3). The difference of the peak positions is about 1 Å. The intramolecular O–H bond length for the SPC model[50] is 1.0 Å. Therefore, the oxygen atom, one of hydrogen atoms in the same molecule, and a surface atom should be in a straight line. The orientation of water molecules at the threefold hollow sites, which is consistent with such a X–H–O configuration should be A or G (see Fig. 2). The difference of the other peak positions in the X–O and X–H correlation functions between these two orientations is small. The peak of the X–O correlation function around 5.2 Å can be assigned to water molecules in the second layer which forms an icelike structure hydrogen-bonded with the molecules (A or G) in the first layer.

Although the difference in the expected positions of the first and second neighbors between the orientations A and G is small, the directions of the dipole moment vector of water molecules in the first and second layer are very different. We define $\theta$ as an angle between the surface normal and dipole moment vectors. When the orientation of the first layer is A, the angle $\theta$ is about 108°. If the icelike structure extends to the second layer, it is predicted that water molecules in the second layer take an orientation similar to E. Therefore, the angle $\theta$ of water molecules in the second layer is about 126°. On the other hand, the angle $\theta$ in the first layer is about 54°, if the molecular orientation is G. In this case, it is predicted that those in the second layer are similar to C for which angle $\theta$ is about 72°. The interaction energy between the surface and water molecules is much higher in G and C than in A and E because the surface charge is negative and the angles in C and G are less than 90°. Therefore, we conclude that the orientation of molecules in the first layer is A.

The orientation assigned to water molecules in the first layer agrees with that proposed experimentally by the surface enhanced infrared absorption spectroscopy applied to the Au(111) surface in aqueous solutions of perchloric acid (SEIRAS).[17] If the orientation of water molecules in the first layer is G, the hydrogen-bonded O–H stretching band must be observed by SEIRAS, because the absorption intensity is roughly proportional to $\cos^2 \phi$ (the surface selection rule of SEIRAS), where $\phi$ is the angle between an oscillating dipole and the surface normal vector. The O–H stretching band generally becomes broad and is redshifted when an H atom is engaged in the hydrogen bond. However, the observed O–H stretching band at the surface with negative charges does not show such an indication of hydrogen bonding. Therefore, the orientation G is not consistent with the SEIRAS experiment.

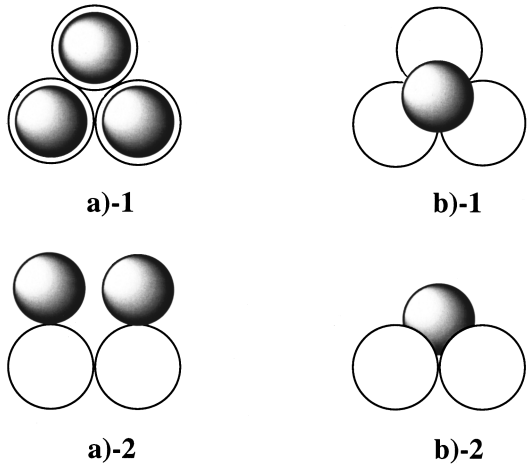


FIG. 4. Adsorption sites. White and shaded spheres are surface atoms and adsorption molecules, respectively. (a)-1. On top sites (top view). (a)-2. On top sites (side view). (b)-1. Threefold hollow site (top view). (b)-2. Threefold hollow site (side view).

According to the results of molecular simulations of water molecules on a Pt(100) surface, the orientation of water molecules in the first layer is A-like,[36,37] which is consistent with our result. However, oxygen atoms of the water molecules are found on top of the surface atoms in contrast to our results in which oxygen atoms are located in the threefold hollow sites. It is of interest to carry out a molecular simulation for the water–Au(111) system in order to investigate the cause of the difference.

### 2. Neutral surface

We discuss structure and orientation of water molecules at the uncharged surface. In the case of a neutral wall the correlation functions are solid lines in Fig. 3. We note the peak positions of the X–O correlation functions in the case of a neutral wall are similar to those in the case of a negative wall. Therefore, it is reasonable to make the same assignment for the oxygen position with the case of the negatively charged surface. The atoms in the Au(111) surface and the water-oxygen in the first layer form a closest packed structure. Each water molecule in the first layer is located on the threefold hollow site (see Fig. 4). However, those peaks are not as prominent as in the case of the negatively charged surface, namely, the position and orientation of water molecules are less well-defined than those in the negatively charged wall. The X–H correlation function has no distinct peaks, which indicate that there is no preference in the orientation of water molecules at the surface.

The orientation B has been assigned by SEIRAS to water molecules in the first layer at the neutral surface based on the low intensity of infrared absorption, which should be greater if the surface selection rule is satisfied.[17] When the orientation is B and there is no preference in orientation about the axis perpendicular to the surface, the X–H correlation function would have little structure. Our results for the neutral surface do not exclude the orientation assigned by the SEIRAS experiments although some ambiguity still remains.

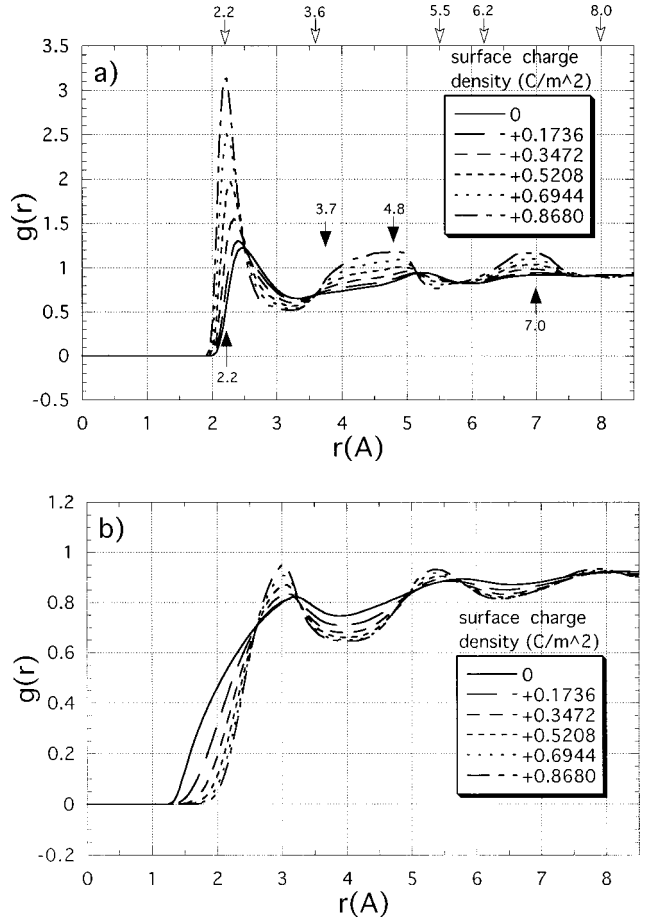


FIG. 5. The correlation functions between a surface atom (X) and water molecules at neutral and positively charged Au(111)-like surface (Type 1). (a) Surface atom (X)–oxygen correlation functions. If oxygen atoms of water molecules are placed on top of the surface atoms (X), it is predicted that the peaks appear around 2.2, 3.6, 5.5, 6.2, and 8.0 Å (marked by white arrows). On the other hand, it is predicted that the peaks appear around 2.2, 3.7, 4.8, and 7.0 Å (marked by black arrows), when the atoms in Au(111)-like surface and the water-oxygen atoms in the first layer form the closest packed structure. (b) Surface atom (X)–hydrogen correlation functions.

### 3. Positively charged surface

Figure 5 shows the correlation functions in the case of a neutral and positively charged wall. The main feature of the X–O correlation functions is the drastic increase in the height of first peak which becomes more and more prominent as the surface charge becomes larger. The peak position is at slightly shorter distance than those of a negatively charged or neutral surface. In the case of surface charge density, $+0.868\ \mathrm{Cm}^{-2}$, the first peak exists around 2.2 Å. It is predicted that the peaks should appear around 2.2, 3.6, 5.5, 6.2, and 8.0 Å, if oxygen atoms of water are placed on top of the surface atoms (marked by white arrows). However, there is no peak and no shoulder around 5.5, 6.2, and 8.0 Å. On the other hand, it is predicted that the peaks appear around 2.2, 3.7, 4.8, and 7.0 Å (marked by black arrows), when the atoms in the Au(111) surface and the water-oxygen in the first layer form a closest packed structure. Those positions are in good agreement with the peak positions of the correlation function. Therefore, the latter in which each water molecule

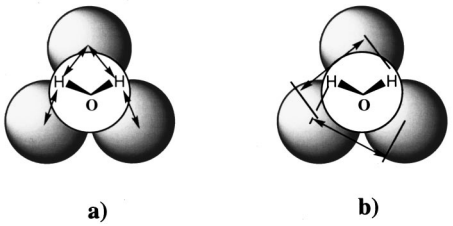


FIG. 6. Top view of the O–H bond directions in a water molecules whose orientation is C (see Fig. 2) in the first layer. Three shaded spheres are surface atoms. White spheres, which are located on the threefold hollow sites, are water-oxygen atoms in the first layer. (a) The number of the nearest positions (indicated by arrows), which is at 2.7 Å from each atom in Au(111) surface, available for H atom of water molecule located at the threefold hollow site is four. (b) The number of second nearest position per one hollow site at 3.4 Å is two.

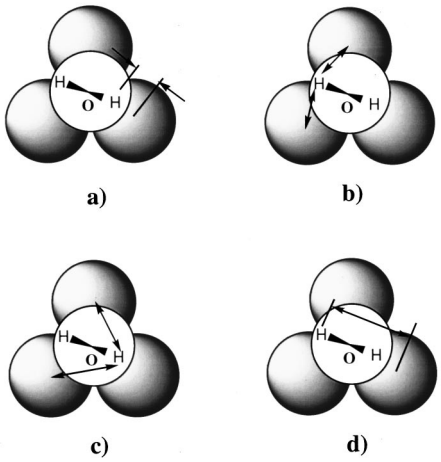


FIG. 7. Top view of the O–H bond directions in a water molecules whose orientation is D (see Fig. 2) in the first layer. Three gray spheres are surface atoms. White spheres, which are located on the threefold hollow sites, are water-oxygen atoms in the first layer. (a) The number of the nearest positions (indicated by arrows), which is at 2.5 Å from each atom in Au(111) surface, available for H atom of water molecule located at the threefold hollow site is one. (b) The number of the second nearest position per one hollow site at 2.8 Å is two. (c) The number of the third nearest position per one hollow site at 3.2 Å is two. (d) The number of the fourth nearest position per one hollow site at 3.5 Å is one.

of the first layer is located on threefold hollow sites is assigned to the oxygen atoms at the positively charged surface.

In Fig. 5(b) we show the X–H correlation functions in the case of positively charged wall. The results exclude the possibility of all other orientations than C and D in Fig. 2, because those orientations should give a greater population of H atom at distance less than 2.2 Å. The X–H correlation functions have the first peak around 3.0 Å. However, the positions of hydrogen atoms in the nearest neighbor are expected to be around 2.5 and 2.7 Å when the orientations are D and C, respectively. Why is the first peak around 3.0 Å? The question can be answered by counting up all possible X–H distances consistent with the C and D configurations. When the orientation is C, the directions of water molecules in the first layer are shown in Fig. 6. Oxygen atoms of water molecules in the first layer are located on the threefold hollow site. Hydrogen atoms are at the positions equally separated from two atoms in the Au(111) surface as illustrated in Fig. 6. The number of the nearest positions available for H atoms of water molecules, which is at 2.7 Å from each atom in the Au(111) surface is four [see Fig. 6(a)], while that of the second nearest positions (3.4 Å) is two [see Fig. 6(b)]. When the orientation is D, the directions of O–H bonds of water molecule in the first layer are shown in Fig. 7. The numbers of the first, second, third and fourth nearest positions per a hollow site, which are located at 2.5, 2.8, 3.2, and 3.5 Å, are one, two, two, and one, respectively (Fig. 7). A superposition of those configurations with different X–H distances ranging from 2.5 to 3.5 Å gives rise to the peak at 3.0 Å in the X–H correlation functions.

According to the SEIRAS experiment, the orientation of water molecules in the first layer is B at the potential of zero charge (pzc) and the hydrogen end of water becomes more oriented toward the solution phase as the potential increases.[17] Then the orientation is likely to be C at a positively charged surface. At very positive potentials where perchlorate ions adsorbs, the water molecules further reorient toward D due to the coadsorption of perchlorate ions. It is of interest to carry out a RISM calculation applied to Au(111) surface in aqueous solution of perchloric acid in order to investigate effects of ions, especially coadsorption effects.

### B. Type 2 (flatlike surface)

Figure 8 shows the surface atom X–solvent correlation functions at neutral and negatively charged surfaces which are flatlike structure (Type 2). The surface charge-densities are the same as those of Type 1 (Fig. 3). First, the X–O correlation functions are shown in Fig. 8(a). The X–O correlation function does not depend too much on the surface charge-density. The peaks of the correlation function are not as prominent as those of Au(111) surface although the nearest neighbors are placed around 2.5 Å. It is concluded that there is little preference in the direction parallel to the surface and that the water molecules are not located on the specific sites.

In contrast to the X–O correlation function, peaks of the X–H correlation functions become more and more prominent as the surface charge density is increased. We note that the X–H correlation functions have first peaks around 1.5 Å in the case of the negatively charged surface. The position of the first peak is shorter than that of the X–O correlation function. The difference in the first neighbor positions is about 1 Å. Therefore, the oxygen atom, one of the hydrogen atoms in the same molecule and the surface atom should be in a straight line. However, there is no hollow site where a water molecule fits in, in this case. Therefore, the angle between the surface normal and one of the O–H vectors must be about 180°. Consequently, the orientation of water molecules in the first layer is E. The second and third neighbor positions of hydrogen atoms expected from the orientation E are consistent with the peak positions of the X–H correlation functions. The orientation assigned to water molecules in the first layer agrees with that proposed by an RHNC study applied to a system consisting of a large sphere and water molecules.[29]

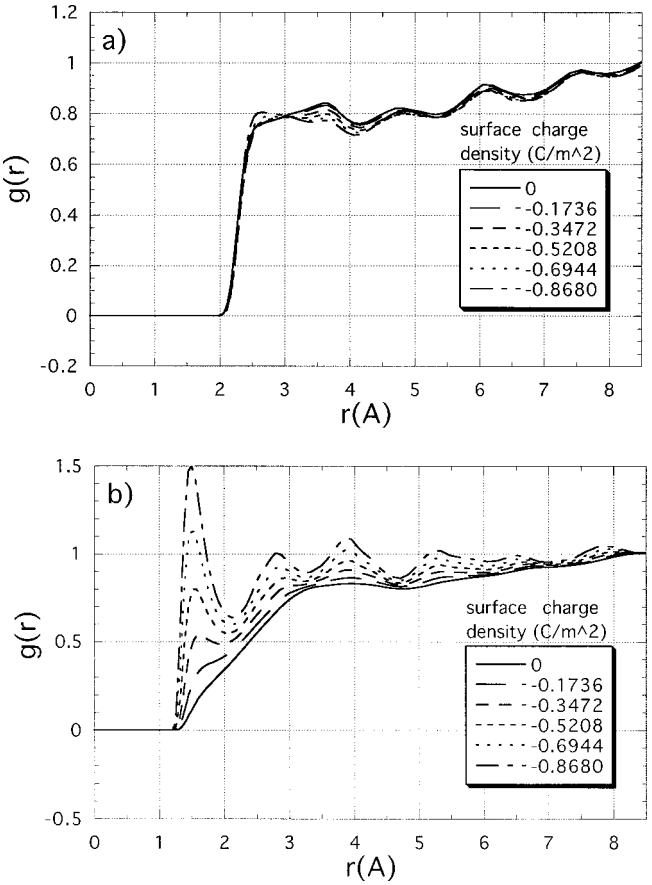


FIG. 8. The correlation functions between a surface atom (X) and water molecules at neutral and negatively charged flatlike surface (Type 2). (a) Surface atom–oxygen correlation functions. The structure of correlation function is not as prominent as in the case of Type 1 (see Fig. 3). (b) The first peak in the X–H correlation function is located at shorter distance than in the X–O correlation function. The difference of the peak positions is about 1 Å.

In the case of positively charged and neutral walls, we could not assign the correlation functions to the orientation of water molecules due to the much less defined structure in the X–H correlation functions. The population of water H atoms in between surface atom and water O atoms is extremely low, which suggests that hydrogen atoms should be directed toward the solution phase. Those results mean that the angle between surface normal and the O–H vector is less than 90°. Therefore, our results are in accord with RHNC,[29] RISM[31] and molecular simulation studies[35] which claim the predominance of the icelike structure near the flat surface with neutral and positive charges.

## V. CONCLUSION

Liquid structures of water at the electrode–solution interface were investigated by RISM integral equation, putting special stress on the effect of surface structure. Two types of surface geometry were examined: Au(111)-like geometries which are characterized by threefold hollow sites in which a water molecule can fit, and a flatlike surface geometry. The orientation of water molecules in the vicinity of surface depends strongly on the surface structure. Especially, the difference is significant in the case of a negatively charged surface. At the Au(111)-like surface with negative charges, angles between the surface normal and both of the two O–H vectors are around 108° (orientation A in Fig. 2). The result agrees with that proposed experimentally by surface enhanced infrared absorption spectroscopy (SEIRAS) applied to the Au(111) surface in aqueous solutions of perchloric acid. On the other hand, in the case of a flatlike surface, the angle between the surface normal and one of the O–H vectors is 180° (orientation E in Fig. 2), H-atom is available for hydrogen-bonding with bulk water.

In the present study, the hydrogen end of water becomes more oriented toward the solution phase above the potential of zero charge (pzc). Those features qualitatively agree with results proposed by the SEIRAS experiment. However, the orientation of water molecules undergoes significant changes due to the coadsorption of perchlorate ion at a surface with very positive potential. A RISM calculation for aqueous solutions of perchloric acid in contact with an electrode is in progress in our group.

## ACKNOWLEDGMENTS

The authors would like to thank Professor Masahiro Kinoshita, Professor Masatoshi Osawa, and Dr. Ken-ichi Ataka for the useful discussions. The authors are grateful to Dr. Hirofumi Sato for his help in computations and discussions. R.A. is supported by Research Fellowships of the Japan Society for the Promotion of Science for Young Scientists. This work was partially supported by Grant-in-Aid for Scientific Research on Priority Area of ''Electrochemistry of Ordered Interfaces'' (No. 09237265) from the Ministry of Education, Science, Sports and Culture, Japan.

[1] K. Itaya and E. Tomita, Surf. Sci. **201**, L507 (1988).
[2] X. Gao and M. J. Weaver, J. Am. Chem. Soc. **114**, 8544 (1992).
[3] N. J. Tao and S. M. Lindsay, J. Phys. Chem. **96**, 5213 (1992).
[4] X. Gao, Y. Zhang, and M. J. Weaver, J. Phys. Chem. **96**, 4156 (1992).
[5] R. L. McCarley, Y.-T. Kim, and A. J. Bard, J. Phys. Chem. **97**, 211 (1993).
[6] O. M. Magnussen, J. Hagebock, J. Hotlos, and R. J. Behm, Faraday Discuss. Chem. Soc. **94**, 329 (1992).
[7] G. J. Edens, X. Gao, and M. J. Weaver, J. Electroanal. Chem. **375**, 357 (1994).
[8] L.-J. Wan, S.-L. Yau, and K. Itaya, J. Phys. Chem. **99**, 9507 (1995).
[9] L.-J. Wan, S.-L. Yau, G. M. Swain, and K. Itaya, J. Electroanal. Chem. **381**, 105 (1995).
[10] S.-L. Yau, Y.-G. Kim, and K. Itaya, J. Am. Chem. Soc. **118**, 7795 (1996).
[11] K. Kunimatsu and A. Bewick, Indian. J. Technol. **24**, 407 (1986).
[12] K. Kunimatsu, M. G. Samant, and H. Seki, J. Electroanal. Chem. **258**, 163 (1989).
[13] M. Osawa, K. Ataka, K. Yoshii, and T. Yotsuyanagi, J. Electron Spectrosc. Relat. Phenom. **64/65**, 371 (1993).
[14] M. Osawa, K. Yoshii, K. Ataka, and T. Yotsuyanagi, Langmuir **10**, 64 (1994).
[15] M. Osawa and M. Ikeda, J. Phys. Chem. **95**, 9914 (1991).
[16] M. Osawa, K. Ataka, K. Yoshii, and Y. Nishikawa, Appl. Spectrosc. **47**, 1497 (1993).
[17] K. Ataka, T. Yotsuyanagi, and M. Osawa, J. Phys. Chem. **100**, 10664 (1996).
[18] C. Gouy, J. Phys. **9**, 457 (1910).
[19] D. L. Chapmann, Philos. Mag. **25**, 475 (1913).
[20] O. Stern, Z. Elektrochem. **30**, 171 (1990).
[21] L. Blum, Adv. Chem. Phys. **78**, 171 (1990).
[22] D. A. Huckaby and L. Blum, J. Chem. Phys. **92**, 2646 (1990).
[23] D. A. Huckaby and L. Blum, J. Chem. Phys. **97**, 5773 (1992).
[24] D. A. Huckaby and L. Blum, J. Electranal. Chem. **315**, 255 (1991).

[25] M. Plischke and D. Henderson, J. Chem. Phys. **88**, 2712 (1988).
[26] D. Henderson and M. Plischke, J. Phys. Chem. **92**, 7177 (1988).
[27] G. M. Torrie, P. G. Kusalik, and G. N. Patey, J. Chem. Phys. **89**, 3285 (1988).
[28] G. M. Torrie, P. G. Kusalik, and G. N. Patey, J. Chem. Phys. **90**, 4513 (1989); G. M. Torrie and G. N. Patey, J. Phys. Chem. **97**, 12909 (1993).
[29] G. M. Torrie, P. G. Kusalik, and G. N. Patey, J. Chem. Phys. **88**, 7826 (1988).
[30] J. P. Valleau and G. M. Torrie, J. Chem. Phys. **81**, 6291 (1984).
[31] M. Kinoshita and F. Hirata, J. Chem. Phys. **104**, 8807 (1996).
[32] D. R. Berard, M. Kinoshita, X. Ye, and G. N. Patey, J. Chem. Phys. **101**, 6271 (1994).
[33] D. R. Berard, M. Kinoshita, X. Ye, and G. N. Patey, J. Chem. Phys. **102**, 1024 (1995).
[34] M. Yamamoto and M. Kinoshita, Chem. Phys. Lett. (in press).
[35] C. Y. Lee, J. A. McCammon, and P. J. Rossky, J. Chem. Phys. **80**, 4448 (1984).
[36] J. Seitz-Beywl, M. Poxleitner, and K. Heinzinger, Z. Naturforsch. Teil A **46**, 876 (1991).
[37] K. Heinzinger, in *Structure of Electrified Interfaces*, edited by J. Lipkowski and P. H. Ross (VCH, New York, 1993), Chap. 7.
[38] P. H. Fries and G. N. Patey, J. Chem. Phys. **82**, 429 (1985).
[39] P. G. Kusalik and G. N. Patey, J. Chem. Phys. **88**, 7715 (1988).
[40] D. Chandler, H. C. Andersen, J. Chem. Phys. **57**, 1930 (1972).
[41] F. Hirata and P. J. Rossky, Chem. Phys. Lett. **83**, 329 (1981).
[42] F. Hirata, P. J. Rossky, and B. M. Pettitt, J. Chem. Phys. **78**, 4133 (1983).
[43] S.-H. Chong and F. Hirata, J. Phys. Chem. **101**, 3209 (1997).
[44] S.-H. Chong and F. Hirata, J. Chem. Phys. **106**, 5225 (1997).
[45] M. Kinoshita and F. Hirata, J. Chem. Phys. **106**, 5202 (1997).
[46] F. Hirata and R. M. Levy, J. Phys. Chem. **93**, 479 (1989).
[47] F. Hirata and R. M. Levy, Chem. Phys. Lett. **139**, 108 (1987).
[48] D. Chandler, Y. Singh, and D. M. Richardson, J. Chem. Phys. **81**, 1975 (1984).
[49] K. S. Schweizer and J. G. Curro, Phys. Rev. Lett. **58**, 246 (1987).
[50] H. J. C. Berendsen, J. P. M. Postma, W. F. von Gunsteren, and J. Hermans, in *Intermolecular Forces*, edited by B. Pullman (Reidel, Dordrecht, 1981).
[51] L. Pauling, in *The Nature of The Chemical Bond*, 3rd ed. (Cornell Univ. Press, Ithaca, New York, 1960).